

CHAPTER - 5

Ultraviolet Photoelectron Spectroscopy (UV-PES)

In UV-PES, the sample is irradiated with light in the vacuum ultraviolet region of the spectrum. The photon source for these measurements is from a gas-discharge tube.

Typical sources employed are shown in Table 5.1.

Table 5.1.

Source	Energy in eV
Helium I (doublet)	21.22
Helium II	40.81
Neon I (doublet)	16.7
Neon II	26.9

These energies are of the same order of magnitude as the binding energies for *valence shell electrons* of molecules and for the valence band states of condensed systems. This means that UV-PES gives information of only the valence orbitals in the molecular systems and possibly the valence band of solids. However, despite the energy limitation, UV-PES has strong advantages in many cases. The probability of photoemission varies with frequency. This can be characterized by the “absorption cross-section for photoemission”. It turns out that this varies approximately as $\nu^{-3.5}$. Hence, excitation in the UV region is easier. In addition, the flux of photons produced by these discharge lamps is intense in comparison to the X-ray sources in X-PES. These factors mean that UV-PES can be more sensitive. It is therefore suited to working with dilute samples, such as gases (using differentially-pumped apparatus to obtain the low pressures required to make PES work, whilst still allowing there to be sufficient gas in the sample chamber) or to adsorbates on solid surfaces. UV-PES is also advantageous when working with delicate samples, as there is less chance of radiation damage. Finally, using UV-PES and varying the irradiating light allows one to see the frequency-dependence of the various PES peaks.

The investigations employing frequency dependence is particularly important for the study of solids. It can be shown on a quantum mechanical basis that the photoemission cross-section depends on the size, number of (angular) nodes and localization of the orbital in question. This means that by repeating the measurement of the PE spectrum with many different exciting radiation energies, one can identify the “d-orbital character” of the orbitals involved. This is useful for assigning bands in solid-state work. It is also an important test of the bonding model which is being used to explain the band structure of the solid in question.

UV-PE spectra can be employed to understand the molecular orbital picture of bonding in molecules. The two molecules of great relevance to catalysis are carbon monoxide and nitrogen. The molecular orbital scheme as well as the corresponding UV-PES spectra for nitrogen and carbonmonoxide are given in Fig 5.1 and 5.2 respectively. It is seen that the HOMO level is a non-bonding (3σ) and the next orbital is strongly bonding (1π) and the third level is again a sigma orbital (2σ) orbital in both the molecules. The UV-PE spectra do not show the deeply bound orbitals since the UP spectra were obtained with only He I light source which has a maximum energy of about 22 eV. It should be recognized that the lone pair electrons are localized on one atom namely C (3σ) and the other (2σ) on another atom, namely on oxygen. In the case of dinitroen, the mixing of atomic orbitals results in 2σ and 3σ having little residual bonding character and they are the conventional “lone pairs” of dinitrogen.

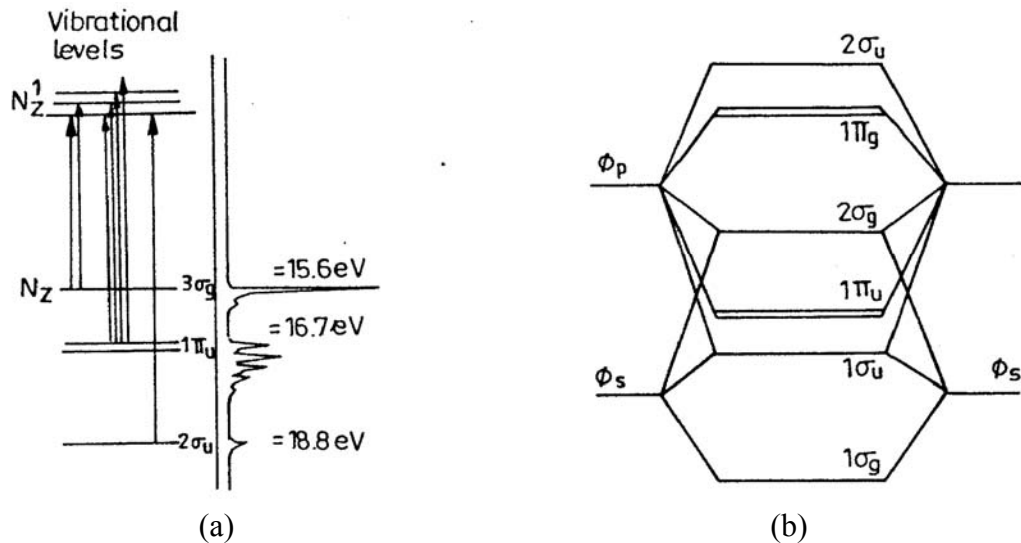


Fig. 5.1 (a) The UV photoelectron spectrum of N_2 . The fine structure in the spectrum arises from the excitation of vibrations in the cation formed by photoejection, (b) the alternative ordering of orbital energies found in homonuclear diatomic molecules from Li_2 to N_2 (Note: Nitrogen atoms have a first ionization energy of 14.5 eV)

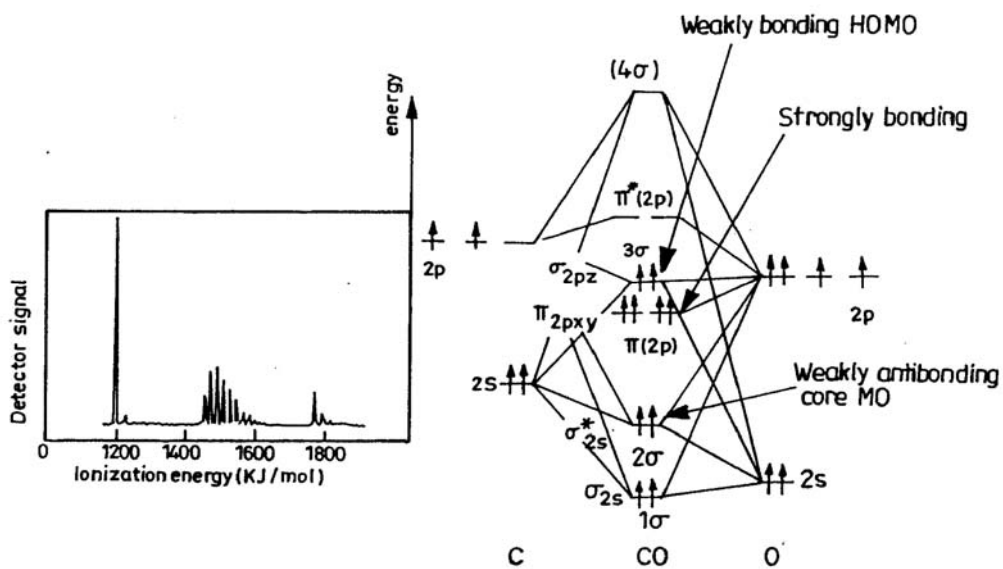


Fig. 5. 2 (Caption need to be given)

Adsorption of gases on metallic surfaces as studied by UV-PES

It is known that the study of the electronic structure of adsorbates is important in understanding the bonding scheme in the adsorbed phase. PES is capable of providing information on the electronic structure of adsorption systems. Since 1970, PES has been extensively used for the study of adsorption of various species on metallic surfaces. However the analysis of spectra of such systems is complicated because of the variations in the interaction between the adsorbate and the metals. It is normally expected that the analysis of the spectra of rare gas atoms adsorbed on metals is simpler because of the weak interaction between the adsorbate and the metal surfaces.

The UP spectra of xenon atoms adsorbed on metal surfaces show two peaks in the region 5-8 eV with respect to the Fermi level which are designated as μ_1 and μ_2 . Typical UP spectra for the adsorption of xenon on W(110) at various coverages are shown in **Fig. 5.3**. The two peaks are usually assigned to the $^2P_{3/2}$ and $^2P_{1/2}$ levels of Xenon atom. The separation between these two peaks is 1.3 eV. In addition the shape of the μ_1 peak is broadened more than is that of the μ_2 peak with respect to those observed for gas phase xenon. However this simple explanation does not take into account the effect of the adsorption phenomenon itself. If one were to consider this bonding effect also, then the 5p orbitals of the xenon atom will be split into 5p σ and 5p π orbitals for the case of interaction of the xenon with the metal surfaces. The resultant ordering of the split energy levels is the same as that obtained with the image potential model. Since the integrated experimental spectra are inadequate for deciding the ordering of the energy levels, the spin resolved photoelectron spectra (SRPES). One such measurement by Schonhense for Xenon adsorption on graphite is shown in **Fig. 5.4**. together with the similar excitation spectra as a function of exposure obtained with EELS(Electron energy Loss spectra) for the Xenon adsorption on gold.

The binding energy or ionization energy shift ΔI , which is defined as $\Delta I = I_{\text{gas}}^v - I_{\text{ads}}^v$ Where I^v is the ionization energy with respect to the vacuum level, is rationalized in terms of an 'initial state' effect ΔI_i (an environment effect caused by the initial interaction) and of a 'final state' effect ΔI_f arising from the relaxation process taking place in the system after the ejection of the outgoing electron. The values of ΔI for a wide variety of substrates are summarized in **Table 5.2** where the substrates are grouped in accordance with their different surfaces: (A) is the bare metal surface (A_0) when $\theta \rightarrow 0$, (A_1) when $\theta \rightarrow 1$; (B) is the second xenon layer; (C) is the first layer of species such as CO, C₂H₂, atomic oxygen and atomic carbon on metal surfaces; (D) is the third xenon layer (D_1) the xenon multilayer beyond the third layer (D_2) or the multilayer of molecular species (H₂O, N₂, CO) (D_3). It is seen from the values that the magnitude of ΔI is of the order of 1-2 eV irrespective of the nature of the metal surface.

Table 5.2 Values of the shifts of the xenon photoelectron spectroscopic peaks (ΔI is the shift in eV, ΔE and ΔE^+ are interaction energies of the ground and ionic state respectively, I_{ads} , I^F are ionization energies with respect to vacuum and Fermi levels respectively ϕ and $\Delta\phi$ are work function for the clean metal and work function change for which coverage $\theta \rightarrow 1$ (monolayer coverage).

(Data reproduced from Ref. S.Ishi and B.Viswanathan, Thin Solid films, **201**, 373(1991).

Substrate	ΔI (eV)	$-\Delta E$ (eV)	$-\Delta E^+$ (eV)	I_{ads} (eV)	I^F (eV)	Φ (eV)	$\Delta\phi$ (eV)
(A ₀)ML $\theta \rightarrow 0$							
Ni(100)	1.27	0.24	1.51	12.13	6.83	5.30	
Pd(111)	0.98	0.36	1.34	12.42	6.47	5.95	
Ag(111)	1.02	0.23	1.26	12.38	7.62	4.76	
W(110)	1.17	0.19	1.36	12.23	7.13	5.10	
Pt(111)	1.10	0.31	1.41	12.30	5.90	6.40	
Al(111)	1.18			12.22	7.74	4.48	
(A ₁) $\theta \rightarrow 1$							
Ni(100)	1.65	0.23	1.88	11.75			0.38
Pd(111)	1.55	0.35	1.90	11.85	6.75		0.85
Ag(111)	1.49	0.25	1.74	11.91			0.47
W(110)	1.52	0.19	1.71	11.88			0.35
Pt(111)	2.26			11.14			0.60
Al(111)	1.80			11.60			0.29
(B) 2 ML							
Ni(110)	1.30			12.10	8.30		0.75
Pd(111)	0.83			12.57	7.47		0.85
Ag(111)	0.96	0.17	0.1.13	12.44	8.15		0.47
W(110)	0.99	0.14	1.13	12.41	7.66		0.35
Pt(111)	1.63	0.21	1.84	11.77			0.60
Al(111)	1.30			12.10	8.20		0.29

(C)							
CO/Ni(110)	0.80			12.50	6.30		-1.65
CO/W(110)	1.89			11.51	5.6		-0.55
C ₂ H ₂ /Pd(100)	1.27			12.13	7.28		0.80
O/W(110)	1.14			12.26	6.26		-0.90
C/Pt(111)	1.91			11.49			
(D ₁) 3 ML							
Ni(110)	1.20			12.20	8.50		0.85
Pd(100)	1.04	0.19	1.23	12.36	7.80		1.09
Ag(111)	0.86	0.15	1.01	12.54	8.33		0.55
Al(111)	1.10			12.30			
(D ₂) Multilayer							
Pd(100)	1.04			12.50			
(D ₃)							
N ₂ /H ₂ O/Ni(110)	1.15			12.55	8.8		1.10
N ₂ /CO/Ni(110)	0.85			12.55	6.35		-1.65

When xenon atoms approach metal surfaces, it is expected that the degenerate 5p orbitals can be resolved owing to interaction with the metal surfaces. The electronic configuration of the ground state of a free xenon atom is $\dots(5p)^6$. The 5p orbitals of xenon on adsorption give rise to two states designated as $5p\sigma$ and $5p\pi$. In this description one assumes that the metal possess a large number of electrons with suitable energy and symmetry for formation of molecular orbital and the metal levels in the ground state is filled up to the Fermi level. Therefore the electronic configuration of adsorbed xenon is given by $\dots(5p\sigma)^2(5p\pi)^4$. the monoionic states possible for xenon have the configurations $(5p\sigma)^1(5p\pi)^4$ with a $^2\Sigma$ or $(5p\sigma)^2(5p\pi)^3$ $^2\pi$ State. The $^2\pi$ state can further split owing to spin orbit interactions into two degenerate states $^2\pi_{1/2}$ and $^2\pi_{3/2}$. The relative ordering of these two states can be either be $E(^2\Sigma) < E(^2\pi)$ or the reverse depending on the magnitude of the interaction. This shows that the assignment of the peaks in UV-PES spectrum of adsorbed inert gases has to be treated where there is no lateral interaction between the adsorbed molecules.

Physical adsorption of dinitrogen on metal surfaces

The properties of dinitrogen in the physical adsorption state can be expected to be similar to those of the gas phase molecule. The UPS data for molecular nitrogen physisorbed on metal surfaces are given in Table 5.3.

Table 5.3 UPS data for the physical adsorption of molecular nitrogen on metal surfaces (Data from Rao C N R and Ranga Rao G, Surface Science Reports, 13,221(1991).

Substrate	$3\sigma_g$ eV	$1\pi_u$ eV	$2\sigma_u$ eV	$(1\pi_u - 3\sigma_g)$ eV	$(2\sigma_u - 1\pi_u)$ eV	T(K)
Gas phase dinitrogen	15.6	17.0	18.8	1.4	1.8	-
Cu (Condensed N ₂)	11.1	12.5	14.3	1.4	1.8	~20
Ni flim	9.7	11.0	12.8	1.3	1.8	7
Ni(111)	9.2	10.5	12.3	1.3	1.8	45
Pd(111)	8.7	10.3	11.9	1.6	1.6	45
Al(111)	10.25	11.6	13.5	1.9	1.9	20

The UP spectrum of physisorbed molecular nitrogen consists of three features due to $3\sigma_g$, $1\pi_u$ and $2\sigma_u$ valence orbitals. The peak separations and their relative intensities are the same as in the gas phase. All the energy levels are, however, shifted to lower binding energies by $\sim 1-2$ eV due to relaxation in the final state.

In the chemisorption of molecular nitrogen on metal surfaces, two states have been identified namely, the weakly adsorbed γ state (end-on orientation) and the strongly adsorbed α state (Side-on orientation). The characteristic features of these states are summarized in Table.4. In the UV photoelectron spectrum the gamma state generally shows two features with the low energy feature containing both $3\sigma_g$ and $1\pi_g$ emission. The alpha state seems to exhibit a three peak spectrum as shown in Table 5.4.

Table 5.4 UP photoelectron spectra of molecular nitrogen chemisorbed on metals.
[Data extracted from Rao C N R and Ranga Rao G, Surface Science Reports, 13,221 (1991).]

Surface	$3\sigma_g$	$1\pi_u$	$2\sigma_u$	T(K)
γ state				
Ni(100)	7.6	-	12.4	77
Ni(111)	9.0	-	13.0	70
Fe(111)	8.6	8.3	11.8-12.2	<77
W(110)	7.0	-	11.7	100
α state				
Fe(111)	8.4	7.5	12.3	110
Cr(110)	8.4	7.1	12.7	90

Composite bands due to ($3\sigma_g + 1\pi_g$) are seen in most cases in the gamma state (weakly chemisorbed state of molecular nitrogen).

UPS studies of Adsorption of carbon monoxide on metallic surfaces

Eastman and Cashion were the first to study the electronic structure of adsorbed CO on nickel surfaces by UPS measurements. Following this study a number of studies dealing with the electronic structure of adsorbed CO on metal surfaces are reported. Eastman and Cashion observed two peaks in the UP spectrum for CO adsorbed on nickel at ~ 7.5 eV and ~ 11.0 eV with respect to the Fermi level of the metal. They assigned these two peaks for emission from 3σ and 1π molecular levels respectively. This initial assignment was not correct. The correct assignment is that the low energy peak is a composite peak for emissions from 3σ and 1π while the peak at ~ 11.0 eV is due to emission from the 2σ level. It has been ascertained that in the adsorbed state the ordering of the energy levels is reversed and that the 1π has a lesser binding energy as compared to the 3σ level though in the gas phase CO the ordering is the reverse. The peak positions of the 3σ , 1π and 2σ levels of CO in the adsorbed state are at 7.84, 7.30 and 10.66 eV respectively. The observed peak positions are given for adsorption of Co on different planes of Group VIII metals in Table.5.

Table 5.5 Peak positions of valence levels with respect to E_F and energy separation for $\tilde{2}\sigma$ and $\tilde{1}\pi$ levels for CO adsorption on group VIII metals [Data adopted from reference, S.S.Ishi *et al.*, Surface Science, 161,349 (1985).]

Substrate	Peak positions				$\Delta(\tilde{2}\sigma - \tilde{1}\pi)$
	$\tilde{3}\sigma$	composite	$\tilde{1}\pi$	$\tilde{2}\sigma$	
Fe(110)		7.5		10.4	2.9
Fe(100)		7.0		10.5	3.5
Fe(111)		7.6		10.8	3.2
Ru(0001)		7.6		10.7	3.1
Co(0001)		7.5		11.0	3.5
Rh(111)	8.3		7.8	11.2	3.4
Rh(100)		7.6		10.8	3.2
Rh(110)	7.6		8.7	10.6	1.9
Ir(111)	9.2		8.6	11.7	3.1
Ir(100)	9.2		8.6	11.5	2.6
Ni(111)	8.1		7.1	11.2	4.1
Ni(100)	8.3		7.8	10.8	3.0
Ni(110)	8.4		6.5	11.7	5.2
Pd(111)	8.2		7.5	11.2	3.7

Pt(111)	9.2		8.4	11.9	3.5
Pt(100)		8.8		11.4	2.6
Pt(110)	9.2		8.2	11.7	3.5
Co (gas)	14.0		16.9	19.7	2.8

Determination of the valence band structure of metals:

The UV-PES can also be employed to determine the electronic structure of metals and deduce the density of states of the valence band of metals. This is feasible since the emission starts from the Fermi level of the metals. In fact the UV PE spectra itself is referenced with respect to the Fermi level of the metallic systems. UV photoelectron spectra obtained for some typical metals like Ni, Cu, Zn and Au and CsAu are shown in Fig.

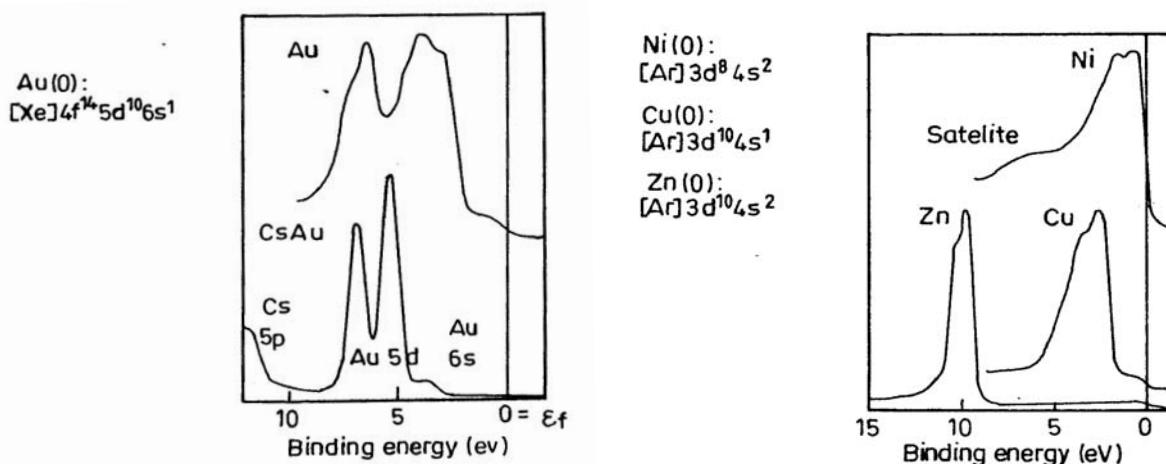


Fig. 5.5.

The points that can be noted are:

1. The nickel Valence band spectrum shows the satellite emission in the energy range around 5 eV which is a characteristic feature of this metal.
2. The copper valence band spectrum shows a shoulder on the higher energy side namely around 3 eV.
3. The Valence band spectrum of Zinc shows not only the higher energy shoulder but also the valence band shows higher binding energy states.
4. The valence band spectrum of gold shows a split pattern which is also present in CsAu system.

In favourable cases the UV-PE spectrum of solids can be used to understand the electronic structure of valence band and also the density of states in this band.

References:

1. Eastman D E and Cashion J K., Phys Rev Lett., 27,1520(1971)
2. S.S.Ishi, Y.Ohno and B.Viswanathan, J.Sci.Ind.Res., 46,541(1987).
3. S.S.Ishi, Y.Ohno and B.Viswanathan, Surface Science, 161, 349(1985).
4. S.Ishi and B.Viswanathan, Thin solid films, 201,373 (1991).
5. C.N.R.Rao and G.Ranga Rao, Surface Science Reports, 13,221 (1991).